Mat. Res. Soc. Symp Proc. 590, 83, 2000

SYNCHROTRON-BASED STUDIES OF TRANSITION METAL INCORPORATION INTO SILICA-BASED SOL-GEL MATERIALS

G. Mountjoy*, D.M. Pickup*, M.A. Holland*, G.W. Wallidge**, R.J. Newport*, M.E. Smith**
*School of Physical Sciences, University of Kent at Canterbury, Canterbury CT2 7NR, U.K.
**Department of Physics, University of Warwick, Coventry CV4 7AL, U.K.

ABSTRACT

Previous structural studies on titania- and zirconia-silica xerogels have shown the occurrence of homogeneous mixing at low metal content, and phase separation at high metal content. The use of additional, complementary, synchrotron-based methods can contribute to a fuller structural description of these materials. We present new X-ray absorption near edge structure (XANES) and SAXS results for $(ZrO_2)_x(SiO_2)_{1-x}$ xerogels and compare them with previous results for $(TiO_2)_x(SiO_2)_{1-x}$ xerogels. Significant differences between $(TiO_2)_x(SiO_2)_{1-x}$ and $(ZrO_2)_x(SiO_2)_{1-x}$ xerogels are observed in the affects of heat treatment on the coordination of homogeneously mixed metal atoms, and in the development of phase separated metal oxide regions.

INTRODUCTION

Mixed titania-silica, $(TiO_2)_x(SiO_2)_{1-x}$, and zirconia-silica, $(ZrO_2)_x(SiO_2)_{1-x}$, materials with low metal content, i.e. $x<0.5$, are potentially useful in a number of technological applications [1,2], including catalysis [3,4]. These materials are also interesting from a structural point of view because the silica network is tetrahedral, but Ti and Zr prefer coordinations greater than 4 [5]. In comparison to high temperature routes, preparation by the sol-gel process [6] has the advantages of using liquid precursors and occurring at low temperatures. However, the structures of xerogels are strongly dependent on the details of preparation and heat treatment.

This paper concerns acid-catalysed $(TiO_2)_x(SiO_2)_{1-x}$ and $(ZrO_2)_x(SiO_2)_{1-x}$ xerogels. Our group has studied the same samples using SAXS [7], diffraction, IR, NMR and X-ray absorption spectroscopies [8,9,10,11 and references therein]. In general, metal atoms are homogeneously incorporated into the silica network at low concentrations, i.e. $x<0.2$, and substantial phase separation of metal oxide occurs at high concentrations, i.e. $x\sim0.4$. This paper focuses on two complementary methods which augment the structural description of these materials. X-ray absorption fine structure (EXAFS) and near edge structure (XANES) probe the local atomic environment of metal atoms, and conversely, small angle X-ray scattering (SAXS) probes mesoscopic-scale inhomogeneities due to phase separation. Here we present new SAXS results for $(ZrO_2)_x(SiO_2)_{1-x}$ xerogels, and compare them with $(TiO_2)_x(SiO_2)_{1-x}$ xerogels [7].

We have previously reported Ti and Zr K-edge EXAFS results for titania- [8,9] and zirconia-silica [10] xerogels (respectively). Table 1 shows selected results for metal-oxygen coordination number N, distance R, and Debye-Waller term $A=2\sigma^2$. In reference compounds, Ti with 4-, 5- and 6-fold coordination has Ti-O distances of 1.81, 1.70/1.99 and 1.96Å respectively [12]. The EXAFS results indicate that for $x<0.2$, Ti has coordination of 4 in heat treated samples, but >4 in unheated samples. In samples with $x\sim0.4$, Ti has a coordination closer to 6. Zr-O coordinations in reference compounds are shown in Table 2. The EXAFS results in Table 1 indicate that for $x\sim0.4$, Zr has coordination of 7. In samples with $x\sim0.1$, the coordination is characterised by a split Zr-O shell, somewhat similar to cubic ZrO_2. However, there remains some ambiguity in the interpretation of the EXAFS results. Here we present new XANES results for $(ZrO_2)_x(SiO_2)_{1-x}$ xerogels, and compare them with $(TiO_2)_x(SiO_2)_{1-x}$ xerogels [7].

Mat. Res. Soc. Symp. Proc. Vol. 590 © 2000 Materials Research Society

Table 1: Metal-oxygen coordination from EXAFS [8,10] in xerogels.

x	heat treat. (°C)	metal-oxygen coordination N	R (Å)	A (Å^2)
$(TiO_2)_x(SiO_2)_{1-x}$				
0.41	none	6.2(10)	1.87(1)	0.05(1)
	750	5.0(6)	1.90(1)	0.022(5)
0.18	none	5.5(10)	1.84(1)	0.03(1)
	750	4.4(4)	1.81(1)	0.016(3)
$(ZrO_2)_x(SiO_2)_{1-x}$				
0.4	none	7.9(5)	2.14(1)	0.023(2)
	750	7.4(5)	2.12(1)	0.028(2)
0.1	none	3.1(4)	2.00(1)	0.006(1)
		6.4(13)	2.25(1)	0.03(1)
	750	2.4(8)	1.98(1)	0.007(2)
		4.4(17)	2.15(4)	0.04(2)

Table 2: Zr-O coordination in reference compounds [13].

compound	Zr-O coord. N	R (Å)	symmetry
$ZrSiO_4$	4	2.13	tetrahedral
	4	2.27	
tetrag. ZrO_2	4	2.08	tetrahedral
	4	2.38	
cubic ZrO_2	3	2.04	distort. tetrah.
	4	2.28	
mono. ZrO_2	7	2.16	disordered
$Zr(OH)_4$	7	2.14	disordered
zirconolite	7	2.16	disordered
$BaZrO_3$	6	2.09	octahedral
Zr propoxide	2	1.96	distort. octah.
	4	2.18	

EXPERIMENT

Sample Preparation

The $(TiO_2)_x(SiO_2)_{1-x}$ samples were prepared using a two-step hydrolysis procedure with acid catalysis (HCl, pH=1). Firstly, tetraethoxyorthosilicate (TEOS) was prehydrolysed for 2hrs by mixing with water and isopropanol in approximately equimolar ratios. Secondly, Ti isopropoxide, and then water, were added dropwise while stirring, such that the final ratio of alkoxide to water equals 2. The resulting gels were dried in ambient conditions and then under vacuum to produce xerogels. Heat treatment consisted of heating at 5°C/min followed by 2hrs at constant temperature. The $(ZrO_2)_x(SiO_2)_{1-x}$ samples were prepared in the same way, except that the solvent was propanol, and the metal alkoxide was Zr propoxide diluted 1:5 in propanol.

X-ray absorption spectroscopy

X-ray absorption spectroscopy experiments were carried out at the Ti and Zr K-edges on stations 8.1 and 9.2 (respectively) of the SRS, Daresbury Laboratory, U.K. Here we describe the Zr K-edge XANES experiments. Samples of suitable and uniform thickness were prepared by grinding and pressing into pellets. Spectra were collected at the Zr K-edge (17998eV) in transmission mode. At the Zr K-edge, the monochromator resolution is ~5eV, and the limited lifetime of the core-hole causes a broadening of ~2eV [14]. Absorption was measured using standard ion chambers. The XANES spectra were processed in the usual way to obtain normalised absorbance as a function of x-ray energy E [14]. Energies are reported relative to the main inflection point. Experiments at the Ti K-edge (4966eV) were similar [11], except that the energy resolution was ~1eV, the monochromator energy was calibrated during each experiment, and energies are reported relative to the first inflection point of Ti metal.

Small angle x-ray scattering

Here we describe the SAXS experiments for $(ZrO_2)_x(SiO_2)_{1-x}$ xerogels (the SAXS experiments for $(TiO_2)_x(SiO_2)_{1-x}$ xerogels were similar [7]). The SAXS experiments were carried out on station 8.2 of the SRS, Daresbury Laboratory, U.K. X-rays of wavelength λ=1.54Å were used with 4 sets of collimating slits and a camera length of ~4.0m. The angular

scale of scattering is given by $Q=4\pi\sin(\theta/2)/\lambda$, where θ is the scattering angle. Absorption was measured using standard ion chambers. The SAXS was recorded using a quadrant detector. The SAXS detector response was calibrated using a radioactive ^{55}Fe source. The SAXS intensity I(Q) was obtained using standard data reduction techniques.

RESULTS

X-ray absorption spectroscopy

The K-edge XANES spectra for transition metal oxides show characteristic features [15]. The shape of the main absorption peak represents transitions to *p*-type continuum states and "shape resonances" of the metal atom environment. Modelling these using multiple scattering calculations is a very complex endeavour. In many cases, useful qualitative information can be obtained by comparison with reference compounds representing standard coordinations.

The XANES spectra may contain pre-edge peak(s) representing transitions to low-lying states with *pd* mixing. Such transitions are disallowed for completely centrosymmetric metal atom sites, but increase in intensity as the degree of centrosymmetry decreases. The prominence of pre-edge peaks varies for different elements. Ti is an element that exhibits very strong pre-edge peaks, as shown in Figure 1. Furthermore, the height of the pre-edge peak increases from 6- to 5- to 4-fold coordination (denoted $Ti^{[6]}$, $Ti^{[5]}$, $Ti^{[4]}$) due to decreasing centrosymmetry as the coordination changes from octahedral to square pyramidal to tetrahedral, respectively [12]. This approach is put on a quantitative basis by fitting Lorentzians to the pre-edge peak to obtain its relative position and height. Studies of reference compounds have shown that reliable information about Ti coordination can be obtained, as shown in Figure 2 [12].

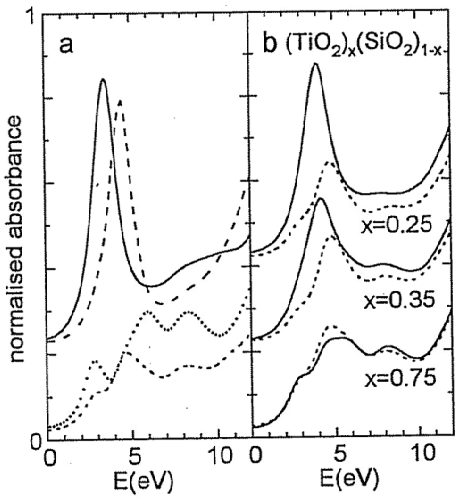

Figure 1: Ti K-edge XANES of (a) $BaTiO_4$, Na_2SiTiO_5, anatase, $ZrTiO_4$ (top to bottom), and (b) $(TiO_2)_x(SiO_2)_{1-x}$ xerogels with x=0.25, 0.35 and 0.75 unheated (dashed) and heat treated at 750°C (solid) [11].

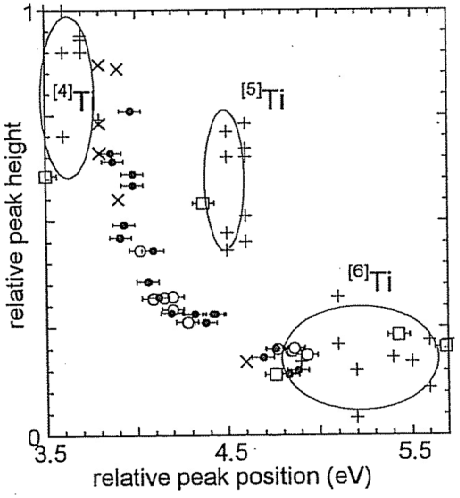

Figure 2: Height and position of pre-edge peak in reference compounds (+ and □), $(TiO_2)_x(SiO_2)_{1-x}$ xerogels prepared with isopropoxide (o) and acetyl-acetone (•) [11], and titania-silica glasses (×) [12,16].

We have used quantitative characterisation of the pre-edge peak to investigate Ti coordination in $(TiO_2)_x(SiO_2)_{1-x}$ xerogels [11]. Typical XANES spectra are shown in Figure 1, and the relative peak positions and heights are shown in figure 2. The results show that xerogels contain a mixture of $Ti^{[6]}$ and $Ti^{[4]}$. Unheated samples contain $Ti^{[6]}$ which is isolated in samples with low x, and in phase separated TiO_2 regions in samples with high x. In samples with low x, heat treatment causes the conversion of isolated $Ti^{[6]}$ to $Ti^{[4]}$, with the loss of hydroxyl and water groups and the substitution of Ti for Si in the silica network. This effect is reduced as x increases because more of the Ti is in phase separated regions, remaining in the form of $Ti^{[6]}$.

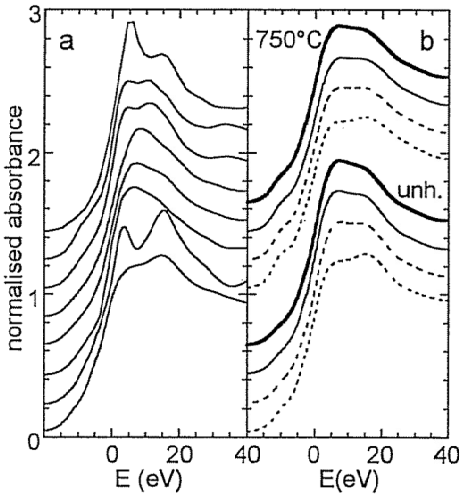

Figure 3: Zr K-edge XANES of (a) $ZrSiO_4$, tetragonal, cubic and monoclinic ZrO_2, $Zr(OH)_4$, zirconolite [13], $BaZrO_3$, Zr propoxide (top to bottom), and (b) $(ZrO_2)_x(SiO_2)_{1-x}$ xerogels with x=0.1(short dash), 0.2 (long dash), 0.3 (thin solid) and 0.4 (thick solid), unheated and heat treated at 750°C.

To obtain information from the XANES spectra of $(ZrO_2)_x(SiO_2)_{1-x}$ xerogels, we compare them with reference compounds, as shown in Figure 3. In samples with x=0.4, the XANES spectra is initially similar to that in $Zr(OH)_4$ and with heat treatment it develops some similarity to that in tetragonal ZrO_2. This implies an amorphous ZrO_2 phase which is initially hydrogenous and develops a local atomic structure similar to tetragonal ZrO_2 (the stable crystal phase of ZrO_2 in small domains). In samples with x=0.1 the XANES spectra are quite different. The unheated samples have XANES spectra similar to that in Zr propoxide rather than the cubic ZrO_2 suggested by EXAFS results. Heat treatment causes the development of a much more prominent pre-edge peak than in any other compounds. Together with the EXAFS results, this implies that Zr has distorted octahedral coordination when mixed into the silica network.

Small angle x-ray scattering

The SAXS intensity, I(Q), contains features due to inhomogeneities in scattering strength, i.e. average atomic number [17]. Xerogel samples are powdered, and typically have packing densities of 50%. Hence, inhomogeneities at the largest length scales are due to powder particles and inter-particle voids. For values of 1/Q which are smaller than the particle size (~μm), but larger than the features within a particle (~nm), the scattering intensity due to particle surfaces is I(Q) is proportional to Q^{d-6}, where the surface "dimension" d is 2 for smooth sharp, surfaces (i.e. Porod scattering) [17], but >2 for rough surfaces, such as observed in clay minerals [18].

Inhomogeneities within xerogel particles arise for at least two reasons. Firstly, acid-catalysed xerogels are microporous [6] and on length scales ≤2nm there is contrast between the silica-based network and pores. Secondly, mixed titania- and zirconia-silica xerogels may contain regions of phase separated metal oxide [e.g. 9,10]. Such phase separated regions may be approximated as independent regions of finite spatial extent, for which I(Q) is proportional to $\exp(-R_g^2Q^2/3)$, where R_g is the radius of gyration [17]. Such scattering causes a shoulder in I(Q) at $1/Q \sim R_g$.

Figure 4 shows the SAXS intensity for $(TiO_2)_x(SiO_2)_{1-x}$ xerogels, with x=0, 0.08, 0.18 and 0.41 [7]. In the samples with x=0 and 0.08 there is no phase separation of TiO_2 (^{17}O NMR spectra show no OTi_n configurations [9], and X-ray absorption spectroscopy shows $Ti^{[4]}$ [11]). The I(Q) show strong Q^{-n} scattering at low Q which is expected due to the surfaces of xerogel powder particles. Interestingly, the values of n are <4, corresponding to rough surfaces, with estimated dimension d=2.35±0.1. The particle surfaces are rough because they are perforated by micropores which permeate the silica-based network. At high Q the I(Q) show a plateau which changes slightly with heat treatment [7]. This feature is due to inhomogeneities within the bulk of the xerogel particles due to micropores.

Having established the SAXS features for homogeneous xerogel samples, we now consider those for phase separation of TiO_2. This occurs in samples with x=0.41 (^{17}O NMR spectra show OTi_n configurations [9], and X-ray absorption spectroscopy shows $Ti^{[6]}$ [11]). The I(Q) clearly have additional intensity in the region of $0.04<Q<0.1Å^{-1}$. With heat treatment the additional intensity becomes more pronounced and moves to lower Q values, corresponding with the formation and growth of anatase crystals. Note that the x=0.18 sample initially has Ti homogeneously mixed in the silica network, but phase separation begins to occur at 750°C due to the reduced solubility of Ti (note that there is no crystallisation at this stage) [7].

Figure 5 shows the SAXS intensity for $(ZrO_2)_x(SiO_2)_{1-x}$ xerogels. The sample with x=0.1 has Zr homogeneously mixed in the silica network (^{17}O NMR spectra show no OZr_n configurations [10]), and the I(Q) is the same as for SiO_2 and $(TiO_2)_{0.08}(SiO_2)_{0.92}$ xerogels. In contrast, the sample with x=0.4 contains substantial phase separated ZrO_2 (^{17}O NMR spectra shows OZr_n configurations [10]). This is apparent in the I(Q) for the unheated sample with x=0.4, and to a lesser extent x=0.3, which have additional intensity in the region $0.06<Q<0.1Å^{-1}$. The I(Q) for the unheated $(ZrO_2)_{0.4}(SiO_2)_{0.6}$ and $(TiO_2)_{0.41}(SiO_2)_{0.59}$ xerogels are very similar. However, after heat treatment the I(Q) for the $(ZrO_2)_{0.4}(SiO_2)_{0.6}$ xerogel shows no strong feature representing phase separation. This indicates that the separate ZrO_2 phase is much less

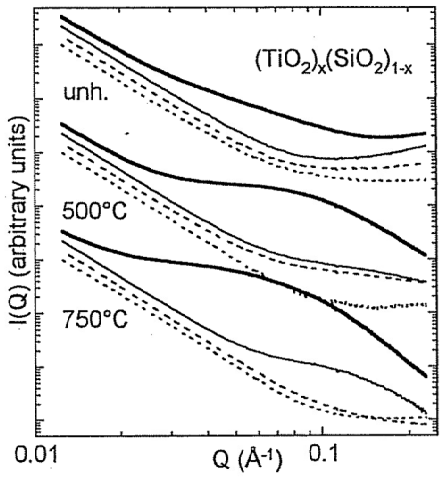

Fig. 4: SAXS I(Q) for $(TiO_2)_x(SiO_2)_{1-x}$ xerogels with x=0 (short dash), 0.08 (long dash), 0.18 (thin solid) and 0.41 (thick solid)

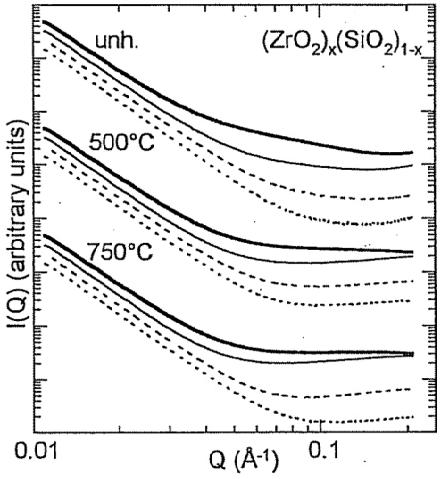

Fig. 5: SAXS I(Q) for $(ZrO_2)_x(SiO_2)_{1-x}$ xerogels with x=0.1 (short dash), 0.2 (long dash), 0.3 (thin solid) and 0.4 (thick solid).

susceptible to consolidation and eventual crystallisation than the separate TiO_2 phase (the former does not crystallise at 750°C, but the latter begins to crystallise at 500°C). The separate amorphous ZrO_2 is hence stabilised by the surrounding silica network.

CONCLUSIONS

The XANES spectra for $(ZrO_2)_x(SiO_2)_{1-x}$ xerogels with x=0.4, in which there is phase separated ZrO_2, indicates the local atomic structure develops with heat treatment from being like that in $Zr(OH)_4$ to like that in tetragonal ZrO_2. The XANES spectra for xerogels with x=0.1, in which Zr is homogeneously mixed into the silica network, indicates that the Zr coordination is initially similar to that in Zr propoxide and remains octahedral after heat treatment. This contrasts with $(TiO_2)_x(SiO_2)_{1-x}$ xerogels with x<0.2, in which Ti coordination is initially octahedral but becomes tetrahedral after heat treatment. The SAXS intensities show that inhomogeneities due to phase separation of metal oxide in both $(TiO_2)_{0.4}(SiO_2)_{0.6}$ and $(ZrO_2)_{0.4}(SiO_2)_{0.6}$ are initially very similar. However, whereas TiO_2 regions undergo consolidation and subsequent crystallisation, this does not happen to ZrO_2 regions which are stabilised by the surrounding silica network.

REFERENCES

[1] P.C. Shultz and H.T. Smyth, in *Amorphous Materials*, edited by Douglas EW and Ellis B (Wiley, London, 1972).
[2] M. Nogami, J. Non-Cryst. Solids **69**, 415 (1985).
[3] M. Itoh, H. Hattori, and K.J. Tanabe, J. Catalysis **35**, 225 (1974).
[4] J.B. Miller and E.I. Ko, J. Catalysis **159**, 58 (1996).
[5] R. Gill, *Chemical Fundamentals of Geology* (Unwin Hyman, London, 1989).
[6] C.J. Brinker and G.W. Scherer, *Sol-gel science: the Physics and Chemistry of Sol-gel Processing* (Academic Press, San Diego, 1990)
[7] G. Mountjoy, J.S. Rigden, R. Anderson, G.W. Wallidge, R.J. Newport, and M.E. Smith, J. Mat. Res. submitted (1999).
[8] R. Anderson, G. Mountjoy, M.E. Smith and R.J. Newport, J. Non-Cryst. Solids **232-234**, 72 (1998).
[9] D.M. Pickup, G. Mountjoy, G.W. Wallidge, R. Anderson, J.M. Cole, R.J. Newport and M.E. Smith, J. Mat. Chem. **9**, 1299 (1999).
[10] D.M. Pickup, G. Mountjoy, G.W. Wallidge, R.J. Newport and M.E. Smith, Phys. Chem. Chem. Phys. **1**, 2527 (1999).
[11] G. Mountjoy, D.M. Pickup, G.W. Wallidge, R. Anderson, J.M. Cole, R.J. Newport and M.E. Smith, Chem. Mater. **11**, 1253 (1999).
[12] F. Farges, G.E. Brown, A. Navrotsky, H. Gan and J.J. Rehr Geochimica et Cosmochimica acta **60**, 3023 (1996).
[13] F. Farges, G.E. Brown, and D. Velde, Am. Mineralogist **70**, 838 (1994).
[14] A. Bianconi, in *X-ray absorption: principles, applications, techniques of EXAFS, SEXAFS and XANES*, edited by Koninbsberger D.C. and Prins R. (Wiley, New York, 1987).
[15] L.A. Grunes Phys. Rev. B. **27**, 2111 (1983).
[16] R.B. Greegor, F.W. Lytle, D.R. Sandstrom, J. Wong and P. Schultz, J. Non-Cryst. Solids **55**, 27 (1983).
[17] LA Feigin and DI Svergun, in *Structure analysis by small-angle X-ray and neutron scattering* (Plenum Press, New York, 1987)
[18] P.W. Schmidt, J. Appl. Cryst. **24**, 414 (1991)